

ELECTRONIC SUPPLEMENTARY INFORMATION (E.S.I.)

A Hybrid Nanoparticle Matrix for Mass Spectrometry

Po-Han Li,^a Shin-Yi Huang,^a Yu-Chie Chen,^{ab*} and Pawel L. Urban^{ab*}

^a Department of Applied Chemistry, National Chiao Tung University;
Hsinchu 300, Taiwan

^b Institute of Molecular Science, National Chiao Tung University;
Hsinchu 300, Taiwan

* Corresponding authors: Prof. Yu-Chie Chen and Prof. P. L. Urban; Fax +886-3-5723764.

ADDITIONAL TABLE

Table S1. Matching the observed and the predicted m/z values after the analysis of *Closterium acerosum* cells by negative-ion MALDI-TOF-MS using 9-aminoacridine as matrix, and in the presence of internal calibrants. The internal calibrant mixture contained adenosine triphosphate, guanosine triphosphate, uridine diphosphate glucose, acetyl coenzyme A and bradykinin acetate (each at the concentration of 8.33×10^{-6} M).

Observed m/z	Predicted formula	Predicted m/z [M-H] ⁻	$ \Delta m $ (Da)
709.379	C ₃₈ H ₆₃ O ₁₀ P	709.40861	0.03
779.510	C ₄₃ H ₇₃ O ₁₀ P	779.48686	0.02
815.500	C ₄₆ H ₇₃ O ₁₀ P	815.48484	0.02

ADDITIONAL FIGURES

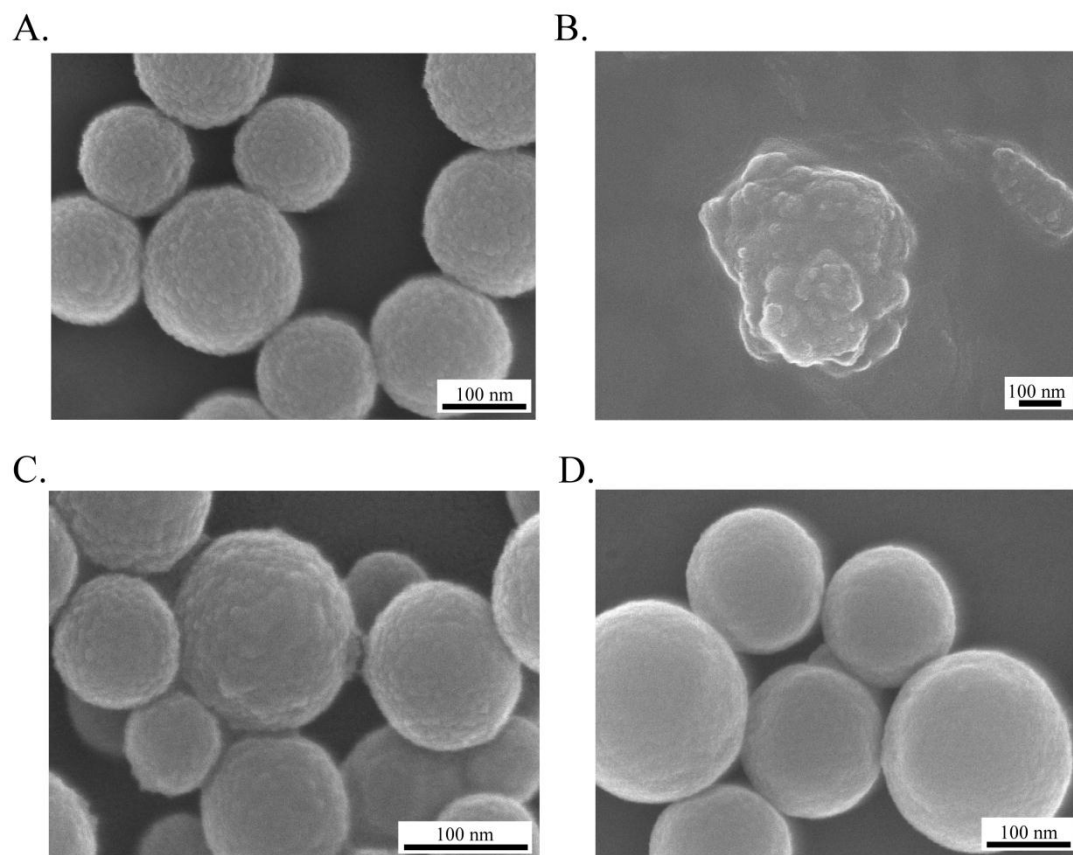


Figure S1. Scanning electron micrographs of the hybrid SiO₂/9-AA nanoparticles (A and B) as well as single-component SiO₂ nanoparticles (C and D). (A) SiO₂/9-AA nanoparticles (as synthesized). (B) SiO₂/9-AA nanoparticles following incubation in NH₃(aq) solution for 30 min. (C) SiO₂ nanoparticles (without 9-AA) synthesized using 3 mL 33% NH₃(aq). (D) SiO₂ nanoparticles (without 9-AA) synthesized using 4 mL 33% NH₃(aq). Comparison of (A) and (B) reveals the influence of NH₃(aq) on the integrity of the hybrid SiO₂/9-AA nanoparticles. Comparison of (C) and (D) reveals the influence of the alkaline component (NH₃(aq)) used as a substrate in the synthesis of SiO₂ nanoparticles on the occurrence of nanoscopic features on their surface.

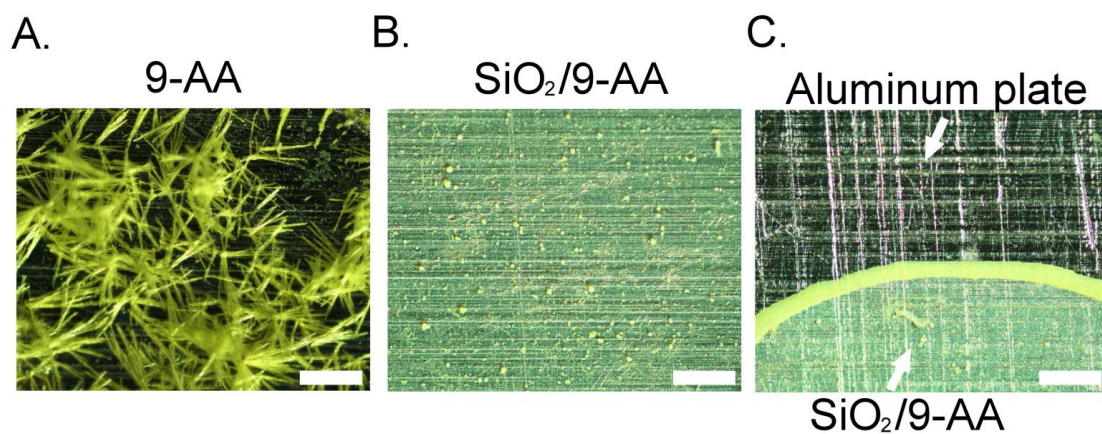


Figure S2. Optical micrographs of dry deposits of different samples on an aluminum plate used as MALDI target: (A) 2 μL of 1:1 (v/v) mixture of 9 mg mL^{-1} 9-AA solution in acetone and 10^{-5} M adenosine triphosphate in water; (B) 2 μL 10^{-5} M solution of adenosine triphosphate was allowed to dry, followed by deposition of 0.5 μL suspension of the $\text{SiO}_2/9\text{-AA}$ nanoparticles (5 mg mL^{-1}). (C) Micrograph showing the edge of the $\text{SiO}_2/9\text{-AA}$ nanoparticle deposit on the aluminum plate (same as in (B)). Hybrid $\text{SiO}_2/9\text{-AA}$ nanoparticles provide relatively good homogeneity of the matrix deposit on the microscopic level (B and C), as compared with the heterogeneous crystalline deposit of 9-AA (A). Scale bars: 200 μm .

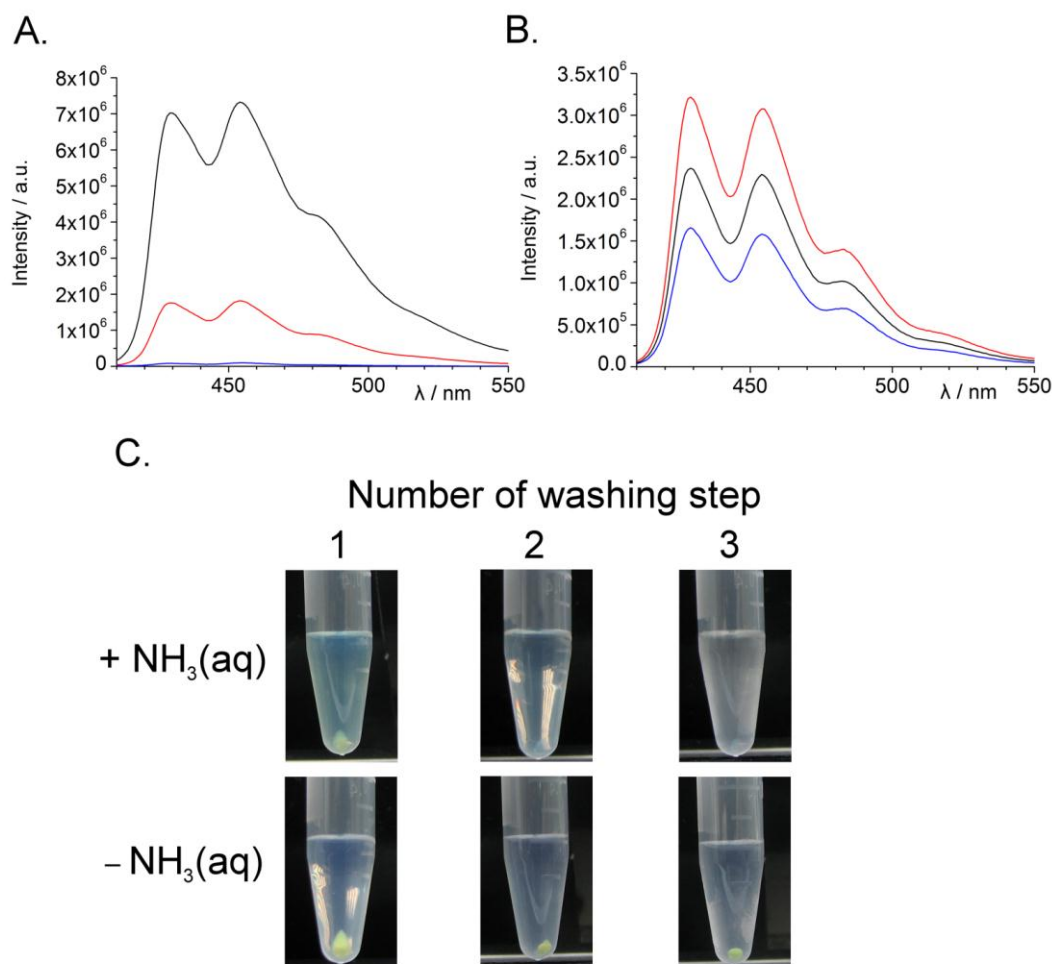


Figure S3. Controlled release of 9-AA in the liquid phase. (A and B) Fluorescence spectra ($\lambda_{\text{ex}} = 400$ nm) of supernatants collected from the SiO₂/9-AA nanoparticle suspensions. (A) Leaching 9-AA from the SiO₂/9-AA nanoparticles by addition of 10 μL of 33% NH₃(aq) to 200 μL of the 0.5 mg mL⁻¹ nanoparticle suspension in 50% ethanol. The pH of the resulting suspension was ~ 14 . (B) Leaching 9-AA from the SiO₂/9-AA nanoparticles with 10 μL of pure water. The black lines in (A) and (B) correspond to the supernatant from the 1st washing step, and the red and blue lines correspond to the supernatants obtained after the 2nd and the 3rd washing step, respectively. (C) Photographs of 0.6-mL microcentrifuge tubes containing SiO₂/9-AA nanoparticles – after washing with NH₃(aq)/water, and centrifugation (10000 rpm, 10 min). Note that the pellets became pale after the treatment with NH₃(aq) (C), which indicates the 9-AA had been leached from the SiO₂/9-AA nanoparticles.

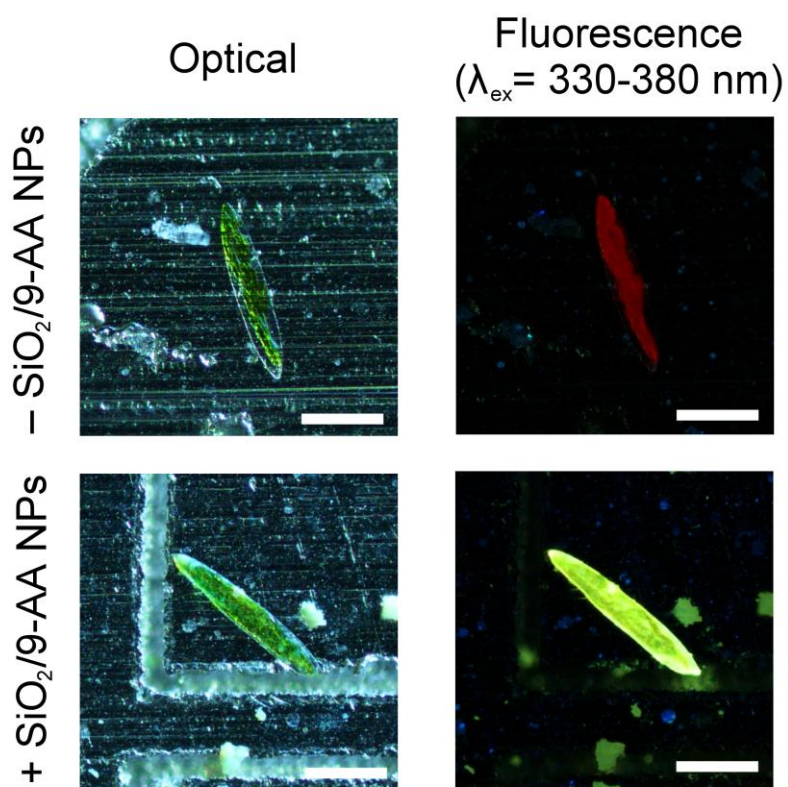


Figure S4. Optical and fluorescence micrographs of individual *Closterium acerosum* cells with/without SiO₂/9-AA nanoparticles. Scale bars: 200 μm .

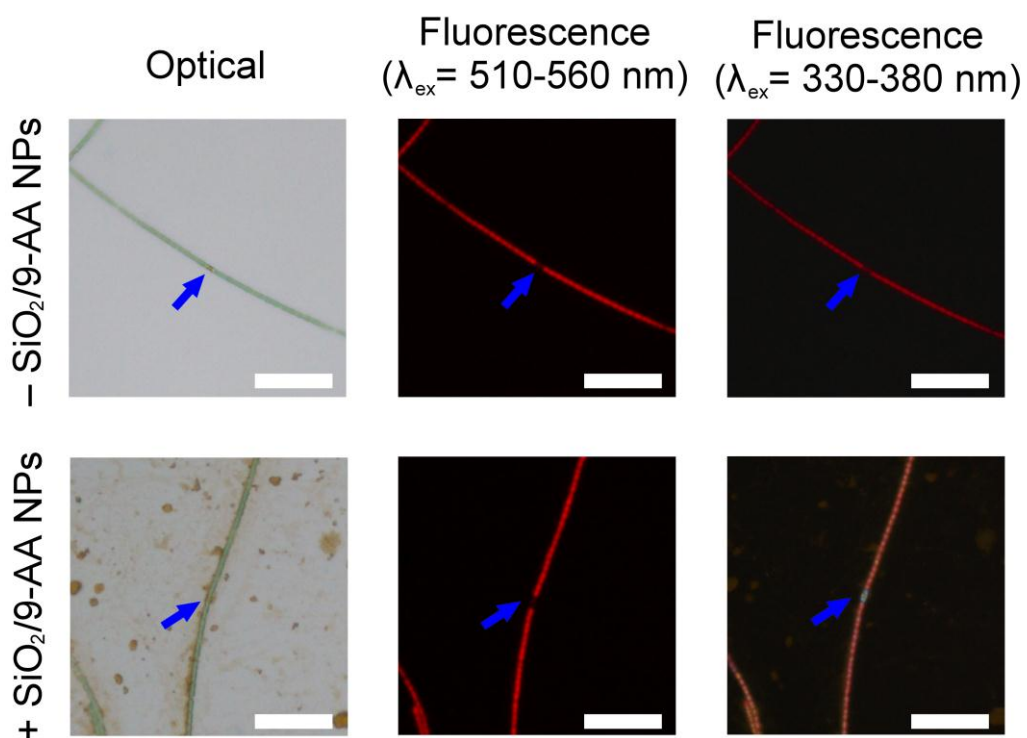


Figure S5. Optical and fluorescence micrographs of *Anabaena* spp. with/without SiO₂/9-AA nanoparticles (0.5 μL , 5 mg mL^{-1}). The fluorescence micrographs were obtained using two different excitation wavelengths ($\lambda_{\text{ex}} = 510-560$ and 330-380 nm – middle and right, respectively). Blue arrows indicate heterocysts. Scale bars in (A): 50 μm .

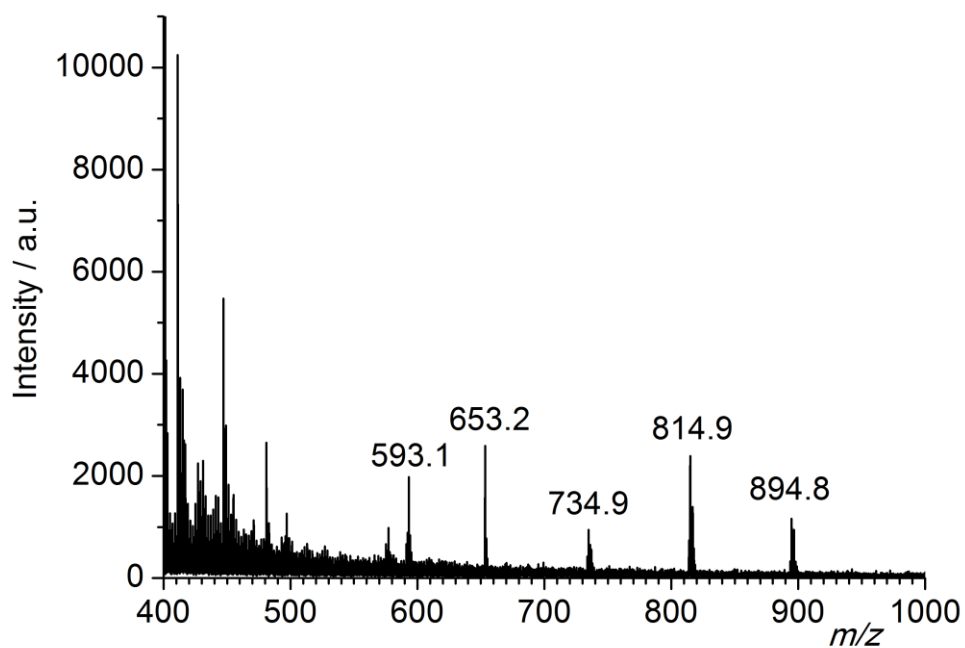


Figure S6. MALDI mass spectrum of SiO₂/9-AA nanoparticles deposited on an aluminum plate, and incubated with gaseous ammonia (blank). Note that the signal at the *m/z*: 814.9 – in this blank spectrum – does not completely overlap with the signal at the *m/z*: 815.5 – recorded when analyzing the sample of *Closterium acerosum* cells (*cf.* **Figure 3B**).

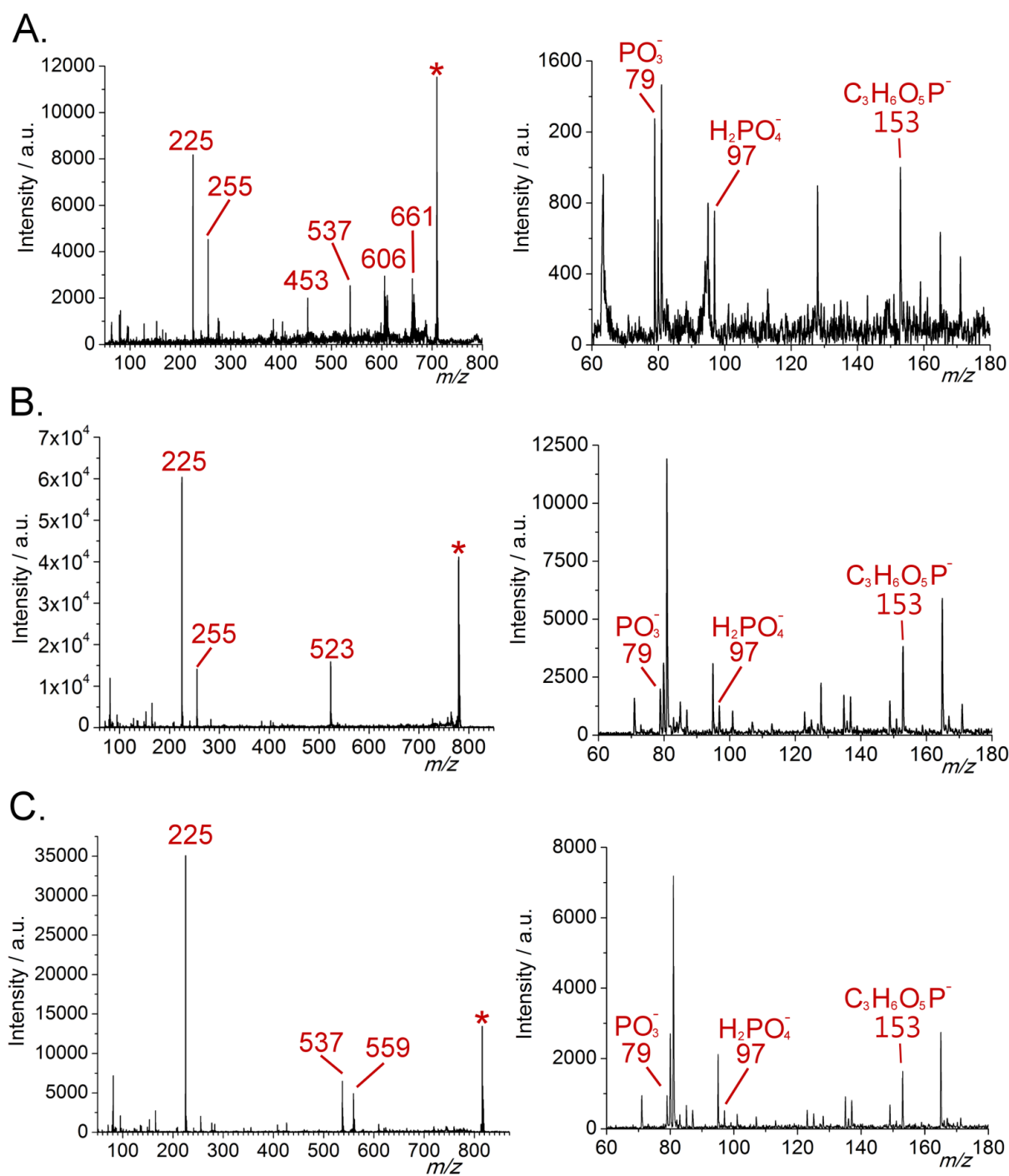


Figure S7. MALDI-MS/MS spectra of the three ions corresponding to the MALDI images depicted in **Figures 3** and **S8**: (A) m/z 709.4, (B) m/z 779.5, (C) m/z 815.5. Precursor ions are marked with asterisks (*). The traces in the left-side column represent full m/z -range spectra whereas the traces in the right-side column display the low- m/z range (within the same spectra). The tandem mass spectra were obtained from the samples of *Closterium acerosum* (co-crystallized with 9-AA) in the negative-ion mode, using the laser-induced fragmentation technology (LIFT).

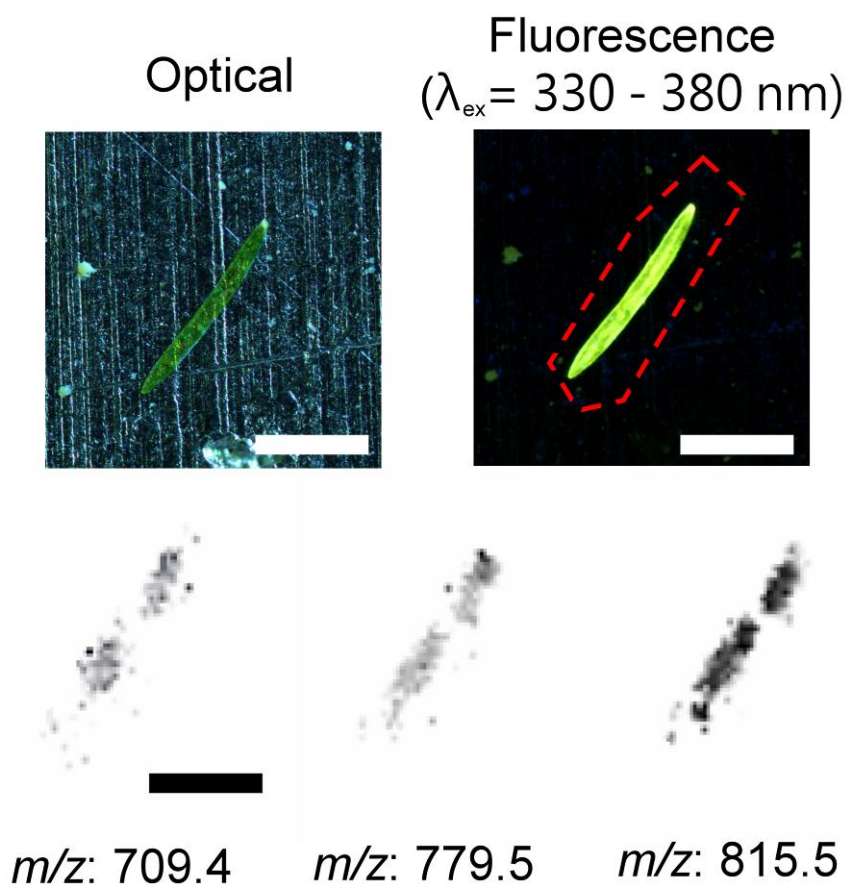


Figure S8. Optical and fluorescence micrographs (top) as well as mass spectrometric images of a single cell of *Closterium acerosum* (bottom). The fluorescence micrograph ($\lambda_{\text{ex}} = 330\text{-}380 \text{ nm}$) shows the presence of $\text{SiO}_2/9\text{-AA}$ nanoparticles (yellow color) on the cell surface (before the exposure to gaseous ammonia). MS images were obtained in the negative-ion mode by MALDI-TOF-MS. Laser beam wavelength: 355 nm; frequency: 50 Hz; diameter: 10 μm ; raster spacing: 10 μm . Scale bars: 200 μm .